Decompression Sickness in Breath-hold diving, and its probable connection to the growth and dissolution of small arterial gas emboli

Saul Goldman, J.M. Solano-Altamirano[1]

Dept. of Chemistry, the Guelph-Waterloo Centre for Graduate Work in Chemistry and the Guelph-Waterloo Physics Institute
University of Guelph, Guelph, Ontario, N1G 2W1, Canada

Abstract

We solved the Laplace equation for the radius of an arterial gas embolism (AGE), during and after breath-hold diving. We used a simple three-region diffusion model for the AGE, and applied our results to two types of breath-hold dives: single, very deep competitive-level dives and repetitive shallower breath-hold dives similar to those carried out by indigenous commercial pearl divers in the South Pacific. Because of the effect of surface tension, AGEs tend to dissolve in arterial blood when in arteries remote from supersaturated tissue. However if, before fully dissolving, they reach the capillary beds that perfuse the brain and the inner ear, they may become inflated with inert gas that is transferred into them from these contiguous temporarily supersaturated tissues. By using simple kinetic models of cerebral and inner ear tissue, the Nitrogen tissue partial pressures during and after the dive(s) were determined. These were used to theoretically calculate AGE growth and dissolution curves for AGEs lodged in capillaries of the brain and inner ear. From these curves it was found that both Cerebral and Inner Ear Decompression Sickness are expected to occur occasionally in single competitive-level dives. It was also determined from these curves that for the commercial repetitive dives considered, the duration of the surface interval (the time interval separating individual repetitive dives from one another) was a key determinant, as to whether Inner Ear and/or Cerebral decompression sickness arose. Our predictions both for single competitive-level and repetitive commercial breath-hold diving were consistent with what is known about the incidence Cerebral and Inner Ear Decompression Sickness in these forms of diving.

Keywords: Growth/dissolution of arterial gas emboli; Breath-hold diving; Diffusion Equation; Cerebral Decompression Sickness; Inner Ear Decompression Sickness.

1. Introduction

This is the 2nd article in which we try to semi-quantitatively predict the rate of growth and dissolution of small arterial gas emboli in relation to the development of particular forms of Decompression Sickness (DCS) that may arise from diving. Our basic strategy is to solve an appropriately written form of the Diffusion Equation for a model of a gas bubble surrounded by a diffusive medium.

In a previous article [1] we compared the exposure and dissolution times of an arterial gas embolism (AGE) in order to establish which AGEs entering arterial circulation through a right-left (r/l) shunt such as a *Patent Foramen Ovale* (PFO), or an arteriovenous anastomosis (AVA), were sufficiently large to reach the Labyrinthine artery in the head before they dissolved. The basic idea was that if they reached this artery before dissolving, Inner Ear Decompression sickness (IEDCS) may occur; otherwise it wouldn't. This, in turn, stems from the generally accepted view that a gaseous seed nucleus in a supersaturated environment is needed to initiate DCS. Among other things, we found that scuba divers with a clinically significant (*i.e.* large) PFO were expected to be particularly vulnerable to IEDCS, even for relatively low-risk dives. This is consistent with clinical observations.

Here we continue with this approach, but apply it to breath-hold diving (*aka* "free-diving"), as opposed to open-circuit scuba diving as in [1]. This extension was made possible by an interesting and very useful recent publication by Fitz-Clarke [2]. In it, Fitz-Clarke derived an arterial gas equation for breath-hold diving, that is applicable at all currently reachable free-diving depths, including depths beyond which total lung collapse occurs in humans (∼233 m).

We also qualitatively assess the likelihood of both Cerebral Decompression Sickness (CDCS) and IEDCS arising after breath-hold diving. By using a simple decompression model to estimate the degree of super-saturation of the brain and the inner ear, we show that CDCS and IEDCS can be expected to occur, at least occasionally, both after a single, deep, competitive-level breath-hold dive, and

Email addresses: sgoldman@uoguelph.ca (Saul Goldman), jmsolanoalt@gmail.com (J.M. Solano-Altamirano)
[1]Corresponding author.

after a series of repetitive breath-hold dives, of the kind done in commercial pearl diving, when the surface interval between the dives is short. This too, is consistent with experience.

Before deriving the mathematical expressions that will provide the radius of an AGE as a function of the variables that underlie the problem (time, external pressure, location in arterial circulation, dive profile), we briefly summarize several issues relevant to DCS and to breath-hold diving. Also, in Section 1.4 we provide an illustrative example on the basis for AGE growth and dissolution that should help to clarify the underlying physical phenomena.

1.1. Breath-hold Diving

Breath-hold and scuba diving differ from one another in a variety of ways, the most obvious being that in scuba diving oxygen is provided to the diver with each breath, while in breath-hold diving the diver's available oxygen is limited to what was in his/her lungs, blood and tissues before starting the dive. They differ also with respect to the lung volume of the diver during the dive, with the volume becoming reduced with depth — to the point of eventual collapse — in breath-hold, but not in scuba diving. Finally, they differ by the onset of the diving-reflex in breath-hold, but not in scuba diving. This is a mammalian physiological reflex, involving a number of changes that support the feasibility of deep breath-hold dives [3]. These changes include a slowing down of the heart rate, and peripheral vasoconstriction that significantly reduces circulation to peripheral tissues, so as to maintain near-normal circulation and perfusion to the heart and the head [2].

1.2. Mechanism underlying the development of CDCS and IEDCS

There is both direct and indirect evidence that CDCS arises when small AGEs enter the capillary network in the brain during decompression, and become inflated with dissolved inert gas that diffuses into the bubbles from the surrounding (temporarily) supersaturated brain tissue. The ischemia that results from the inflated bubble(s) is widely viewed as a likely cause of CDCS. The direct evidence was the observation that the arrival in the brain of arterial gas emboli — observed using a cranial window — coincided with the onset of cerebral dysfunction in severely decompressed dogs [4, 5]. The indirect evidence, like that for a number of other forms of DCS (including IEDCS, spinal DCS, and skin DCS), stems from the positive correlation between the incidence of CDCS, and the existence of a clinically significant PFO in the diver [5].

The evidence that IEDCS stems from small AGEs entering the inner ear, and there becoming inflated during decompression, is entirely indirect. It is (as above) the positive correlation between the incidence rates of IEDCS from unprovocative dives, and the existence of a clinically significant PFO in the divers presenting with IEDCS symptoms [6, 7, 8].

1.3. IEDCS and CDCS in breath-hold diving

Commercial breath-hold diving, if done repetitively and to considerable depths, is believed to occasionally provoke both IEDCS and CDCS. The problem arises relatively frequently when the surface interval between breath-hold dives is short ($\sim$1 min), and it doesn't seem to arise for sufficiently long surface intervals ($\sim$ 15 min) [9, 10]. Symptoms suggestive of IEDCS, (vertigo with accompanying nausea), and CDCS (partial or complete paralysis) were observed in breath-hold pearl divers in the Tuamotu Archipelago near Tahiti. These divers often dove repeatedly to more than 30 msw (100fsw), stayed at the bottom for 30-60 sec, remained underwater for about 1.5 min, and repeated such dives for some 6 hours/day. Their symptoms were locally referred to as "Taravana" ("tara" to fall, "vana", crazily) [3, 9, 10].

Also, two cases of DCS, one involving cerebral neurological symptoms (*e.g.* hemiplegia), and the other both inner ear and cerebral neurological symptoms have been reported for single, breath-hold, competitive-level dives [2]. It was earlier believed that this couldn't happen. This (evidently) mistaken belief was based on the overly simplistic notion that the small amount of Nitrogen in the body during a single (*i.e.* non-repetitive) free dive was insufficient to cause any kind of DCS. As will be shown, the AGEs that act as seed nuclei entering the capillary network of the brain or inner ear can be very small ($O(10\mu)$ in diameter). Consequently, very little Nitrogen is needed to inflate them sufficiently to block the narrow capillaries which perfuse these organs.

1.4. Physical basis for AGE growth and dissolution

An AGE is a gas bubble in arterial circulation. AGEs that arise during and after a dive (both scuba and breath-hold) are believed to originate from venous gas emboli (VGE), that enter arterial circulation because of a variety of not uncommon physiological defects in the body. These defects include cardiac and pulmonary shunts such as PFOs and AVAs, respectively, which shunt venous blood, together with any gas bubbles they contain into arterial circulation. They also include inadequate bubble filtering capacity of the alveoli [1, and references therein].

VGEs form during the decompression phase of a dive, that is, during and immediately after the ascent. They are a consequence of off-gassing of tissues into venous blood. These tissues, which had acquired excess dissolved Nitrogen during the initial compression phase of the dive — descent, and time spent at depth — subsequently release their excess dissolved gas during the decompression phase of the dive, during which they are (temporarily) supersaturated. Venous gas emboli, per se, are not believed to be responsible for most types of DCS, and they are not believed responsible for the types of DCS considered here.

Consider first a small gas bubble in arterial circulation, in the absence of contiguous supersaturated tissue,

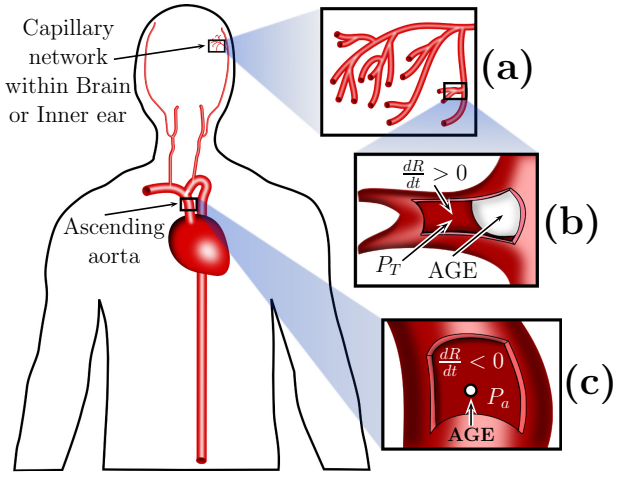

Figure 1: Dissolution and growth of an AGE when travelling from the left atrium in the heart, to the capillary networks of the brain and inner ear. The AGE tends to dissolve when in arteries remote from supersaturated tissue, as in (c). But, as illustrated in (a) and (b), if they reach the capillary beds of either the brain or the inner ear before dissolving, they may become inflated by taking on dissolved inert gas from the supersaturated contiguous tissue surrounding the capillaries. The diameters of these arteries, arterioles and capillaries, are of the order of $10,000\mu$, 50μ, and 10μ respectively.

and with the diver exposed to a constant external pressure, *i.e.* at a fixed depth or at the surface (Fig. 1, Inset c). An AGE under these conditions will dissolve rapidly into its surrounding arterial blood (within seconds or minutes), and doesn't cause DCS. For example, in physiological studies on human subjects with a suspected pulmonary shunt (an AVA) agitated air bubbles suspended in a saline contrast medium were injected into the subjects' cubital vein under laboratory conditions ($\sim$ 1 atm). These bubbles, which were monitored by echocardiography, and were observed to be shunted into arterial circulation after five or more of cardiac cycles, never resulted in DCS [11].

The reason such bubbles dissolve rapidly, and do not cause DCS, is because of the effect of surface tension, which acts to increase the pressure inside a gas bubble, so that its internal pressure exceeds the external (or ambient) pressure. The pressure inside a bubble, for bubbles sufficiently small such that the surface tension cannot be neglected ($R \leq 50\mu$), is given by the Young-Laplace equation:

$$P_b = P_e + \frac{2\gamma}{R} \qquad (1)$$

In Eq. (1), P_b is the total gas pressure inside the bubble, P_e is the external or ambient pressure, γ is the surface tension at the gas/liquid interface of the bubble, and $2\gamma/R$ is the surface tension contribution to the pressure acting on (or compressing) the bubble.

For definiteness, we go through a specific example. Suppose the constant ambient pressure, which equals the total pressure in the lungs, is x atm, and that the mole fraction of Nitrogen in the lungs is f (*e.g.* for air $f \sim 0.79$). The partial pressure of gaseous Nitrogen in the lungs is then fx atm. Alveolar blood equilibrates very rapidly with the gas contents of the lungs, and therefore the dissolved Nitrogen partial pressure of the alveolar blood will also be fx atm, as will be the dissolved Nitrogen partial pressure of arterial blood, whose inert gas content is known to be the same as that of alveolar blood [12]. If the bubble is 10 μ in radius, and the gas/liquid interfacial tension "γ" is 0.7 μ·atm (= 70 dyne/cm, which is the surface tension of water), then, by using Eq. (1), we find

$$P_b = x + (2 \cdot 0.7/10) = (x + 0.14) \text{ atm},$$

and

$$P_b\,(\mathrm{N_2})\,[= f\,(x + 0.14)\,\text{atm}] > P_a\,(\mathrm{N_2})\,[= fx\ \text{atm}]\,.$$

Here $P_b\,(\mathrm{N_2})$ and $P_a\,(\mathrm{N_2})$ are respectively, the gaseous partial pressure of Nitrogen in the bubble, and the dissolved Nitrogen partial pressure in arterial blood. This excess partial pressure of Nitrogen in the bubble, relative to its value in the surrounding arterial blood, will cause gaseous Nitrogen to diffuse out of the bubble and to dissolve in the arterial blood. The imbalance of pressures, and the rate of outward flow of Nitrogen from the bubble will increase, the smaller the bubble. This effect is illustrated in Fig. 1 Inset (c), which shows a bubble under such conditions shrinking with time ($dR/dt < 0$). This will hold true — *i.e.* the bubble will shrink — for an AGE in any part of the arterial network, including arteries, arterioles and capillaries, provided the tissue surrounding the artery/arteriole/capillary is not supersaturated.

The situation changes, however, and the direction of Nitrogen flow relative to the bubble can become reversed, if the AGE doesn't fully dissolve, survives the trip to a capillary, and becomes lodged within it during the decompression phase of the dive. This is illustrated in Fig. 1 Inset (b). The capillary blood next to the bubble is assumed to have the same Nitrogen partial pressure as that of the contiguous tissue (P_T). This assumption is based, both on the very small diameter of the capillary ($O(10)\mu$), and the high permeability of the capillary wall to small (*i.e.* low molecular weight) dissolved solutes [13]. As indicated previously, during the decompression phase of the dive, body tissues become temporarily supersaturated with dissolved Nitrogen. The tissues are supersaturated relative to the Nitrogen content of arterial blood, alveolar blood, and the lungs (all of which will have the same Nitrogen partial pressure). This happens because while the Nitrogen content of arterial and alveolar blood, and of the air space in the lungs, responds very rapidly (essentially immediately) to a change in the ambient pressure, the tissue response time is considerably slower. This is due to the relatively slow tissue perfusion rates that control the rate of tissue on- and off-gassing. Thus, the initial drop in Nitrogen pressure partial (in alveolar blood, arterial blood, and the lungs), that accompanies the drop in ambient pressure during decompression, will exceed the initial drop in tissue

dissolved Nitrogen partial pressure. Consequently, tissues become temporarily supersaturated with dissolved inert gas during decompression. The supersaturation is "temporary", because it is eventually resolved when the tissue has fully off-gassed, and the entire body re-establishes a steady-state.

Again, for definiteness, suppose the diver has just surfaced, the ambient pressure is 1 atm, the tissue contiguous to the capillary has only partially off-gassed, and has a residual dissolved Nitrogen partial pressure of 2 atm, and the bubble has a radius of 10μ. Under these conditions, again assuming that the Nitrogen mole fraction of the gas in the bubble is "f", and that the interfacial tension "γ" is 0.7 μ·atm,

$$P_T\left(\mathrm{N}_2\right)[=2\mathrm{atm}] > P_b\left(\mathrm{N}_2\right)[=1.14f\mathrm{atm}], \quad f \leq 1$$

so that under these conditions the bubble will inflate, *i.e.* $dR/dt > 0$.

More generally, a bubble lodged in a capillary will inflate if $P_T\left(\mathrm{N}_2\right) > P_b\left(\mathrm{N}_2\right)$; otherwise it will shrink and dissolve. Using the condition $P_T\left(\mathrm{N}_2\right) > P_b\left(\mathrm{N}_2\right)$ in Eq. (1), we find the general condition for bubble growth to be

$$R > 2\gamma f/\big(P_T\left(\mathrm{N}_2\right) - P_e f\big).$$

Bubbles for which $R < 2\gamma f/\big(P_T\left(\mathrm{N}_2\right) - P_e f\big)$ will dissolve, since with radii this small, the effect of surface tension, which acts to dissolve the bubble, will outweigh that of supersaturatuon, which acts to inflate it.

2. Theory

We carry out two separate types of calculations. One, described in Section 2.1, is for the AGE radius and internal gas pressure at various points and times while the AGE is in arterial circulation — both within large arteries leading to and in the head, and within the capillaries that perfuse the brain and the inner ear. The second calculation, described in Section 2.2, is for the dissolved inert gas partial pressure in the both brain and inner ear tissue, at all times during and after a dive. For this second calculation the tissues are represented by simplified kinetic models. Both calculations take into account the breath-hold dive profile, *i.e.* the full detailed time-depth course of the single or repetitive breath-hold dive.

2.1. AGE radius and internal pressure

These calculations are similar to those described in [1] for the radius and pressure of an AGE at various locations and times in arterial circulation (during and after a dive), and the reader is referred to this work for additional details. The physical model used here to determine the AGE radius and pressure is shown in Fig. 2.

Three main differences exist between these calculations and those in [1].

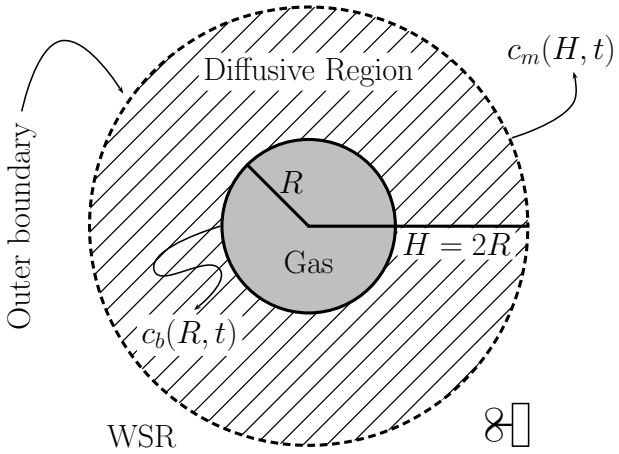

Figure 2: Physical model of a gas bubble surrounded by a diffusive medium, which, in turn, is surrounded by a well-stirred region ("WSR"). In this model, which is a specific version of the LV3 model in [1], the thickness of the diffusive region is taken to be the same as the radius of the bubble (R). The bubble continuously expands or contracts, depending on its location in the circulatory system, and on time.

1. In this work, we use an arterial gas equation appropriate to breath-hold diving, as opposed to one appropriate for scuba diving. These equations provide virtually identical arterial gas pressures (at a given depth) prior to lung collapse, but differ considerably in their predicted arterial gas pressures, after lung collapse.
2. We here solve only the Laplace equation for the desired functions, as opposed to both the Diffusion and the Laplace equations. It was determined in [1] that the simpler Laplace equation was sufficiently accurate for these applications.
3. Here, in addition to the calculation on AGEs circulating in the arteries leading to and in the head, we also include an additional calculation on the approximate time-dependence of the AGE radius and pressure after it is lodged in a capillary bed of the super-saturated brain and inner ear.

In order to render the problem tractable we assume that the AGE is comprised of a single gas, taken here to be pure Nitrogen (*i.e.* $f = 1$ in the equations in Section 1.4), which exchanges with the dissolved Nitrogen in the environment of the bubble.

Fick's law gives the time-evolution of the number of moles of Nitrogen in the bubble:

$$\frac{dn}{ds} = 8\pi R^2 D\left\{s\left(\frac{\partial c}{\partial r}\right)_R\right\}. \tag{2}$$

Here $s \equiv t^{1/2}$ where "t" is time, and $(\partial c/\partial r)_R$ is the radial concentration gradient of dissolved Nitrogen at the surface of the bubble. The variable s is used in order to avoid numerical instabilities at $t = 0$ [1]. Also n, R and D are

respectively the number of moles of Nitrogen gas in the bubble, the radius of the bubble, and the Diffusion Coefficient of dissolved Nitrogen in the medium surrounding the bubble.

The time-evolution of the bubble radius is then obtained by combining Eqs. (1) and (2) with the Ideal Gas Law ($P_b \cdot 4\pi R^3/3 = nBT$). The result is

$$\frac{dR}{ds} = \frac{2s}{3P_e + 4\gamma}\left\{3BTD\left(\frac{\partial c}{\partial r}\right)_R - R^2\frac{dP_e}{dt}\right\}, \quad (3)$$

where B is used for the universal ideal gas constant (to avoid confusion with R, which here denotes the bubble radius).

The expression for the concentration gradient at the bubble surface needed in Eq. (3) is obtained from the Laplace equation, written for spherical symmetry:

$$\nabla^2 c\,(r,t) \equiv \left(\frac{\partial^2 c\,(r,t)}{dr^2}\right)_t + \left(\frac{2}{r}\right)\left(\frac{\partial c\,(r,t)}{\partial r}\right)_t = 0. \quad (4)$$

The resultant solution for the concentration gradient for the LV3 model used here is ([1]):

$$\left(\frac{\partial c}{\partial r}\right)_R = \left(\frac{\lambda}{\lambda - 1}\right)\left(\frac{c_m - c_b}{R}\right) = \frac{2\,(P_x - P_b)}{K_H R}. \quad (5)$$

In Eq. (5) P_x is the dissolved partial pressure of Nitrogen either in an artery or in a capillary, λ is a constant used to represent the time-dependent thickness of the diffusive layer (see Fig. 2, $H(t) = \lambda R(t)$), and K_H is the Henry's law constant for Nitrogen in arterial blood [1]. In this work the dissolved partial pressure of Nitrogen in an artery will be given by the arterial gas equation for breath-hold diving (Eq. (6), below). Its value in a capillary will be assumed to be given by the dissolved Nitrogen partial pressure in the tissue that surrounds the capillary. This, in turn, will be obtained by numerically integrating Eq. (13), below.

2.2. Arterial partial pressure of Nitrogen during a breath-hold dive

We apply the model developed recently by Fitz-Clarke [2], for the arterial partial pressure of Nitrogen during a breath-hold dive:

$$P_a\,(t, z(t)) = P_A(z) - (P_A(z) - P_v)\exp\left(-\frac{D(z)}{\beta Q(t)}\right). \quad (6)$$

In Eq. (6), P_A, P_v, and P_a, respectively represent the alveolar, venous, and arterial partial pressures of Nitrogen, β is the solubility of Nitrogen in blood at body temperature, $D(z)$ is the diffusing capacity of dissolved Nitrogen (below), and $Q(t)$ is the "pulmonary blood flow", which is the amount of blood per unit time passing through the network of vessels between the heart and the lungs. $Q(t)$ is here written with a time-dependence, in order to allow for its depth-dependence in diving (Eq. (10), below).

The alveolar partial pressure of Nitrogen during a breath-hold dive is approximated by [2]

$$P_A = X_{\mathrm{N}_2} P_e(z) = X_{\mathrm{N}_2}\,(1 + Z/33)\,, \quad (7)$$

where z is the depth of the diver (in feet of sea water), and X_{N_2} is the mole fraction of Nitrogen in air (0.79). P_v, the average venous Nitrogen partial pressure for the body as a whole, is assumed to remain constant during the breath-hold dive, with its value throughout the dive given by its value at the surface [2]:

$$P_v = X_{\mathrm{N}_2} P_e(z = 0) = X_{\mathrm{N}_2}\mathrm{atm}. \quad (8)$$

The basis for this approximation is the relatively short duration of any breath-hold dive.

During a breath-hold dive, it is assumed that the pulmonary blood flow $Q(t)$ decreases with increasing depth due to the decreasing diffusing capacity of dissolved Nitrogen. The diffusing capacity of dissolved Nitrogen is denoted as $D(z)$, and is taken as directly proportional to the relative alveolar area:

$$D(z) = D_0 A_L/A_0 = D_0\left((1+\alpha)\,P_e^{0.77} - \alpha P_e^{1.2}\right). \quad (9)$$

Here D_0 is the value of $D(z)$ at the surface, and alpha is a fitted constant. The values of the exponents given in the expression for the relative alveolar area (A_L/A_0) were previously determined by fitting to open-circuit scuba DCS risk data (see Ref. [2]).

The pulmonary blood flow , needed in Eq. (6), will be determined from the rate of pulmonary blood flow:

$$\frac{dQ(t)}{dt} = \frac{1}{\tau_{DR}}\Big\{(Q_s - Q_o)\exp\left(-K_{DR} z(t)\right) + Q_o - Q(t)\Big\}. \quad (10)$$

In Eq. (10), Q_s is the initial value of the pulmonary flow at the surface, and Q_o is the minimum pulmonary flow under dive reflex activation. As shown in Eq. (10), the pulmonary blood flow rate involves depth and time constants (K_{DR} and τ_{DR}) [2].

We have found that for linear ascents and descents, *i.e.*, for dives with constant ascent/descent rates, the pulmonary blood flow $Q(t)$ can be obtained in closed form by analytically integrating Eq. (10). For linear ascents/descents, the depth follows the time-dependence

$$z(t) = z_0 + \dot{z}\,(t - t_0)\,. \quad (11)$$

Here $\dot{z}$ is the constant descent/ascent rate. Constant descent/ascent rate breath-hold dives can be described by a piece-wise continuous function, with each stage of the dive (descent, rest or stop, and ascent) captured by the general form given by Eq. (11). By using Eq. (11) for $z(t)$ in Eq. (10), the integrated expression for the pulmonary blood

flow is found to be

$$\begin{aligned} Q(t) &= Q_o\left(1-\exp\left(-\left(t-t_0\right)/\tau_{DR}\right)\right) \\ &\quad +\frac{Q_s-Q_o}{1-\tau_{DR}\dot{z}K_{DR}}\exp\left(-K_{DR}z_0\right) \\ &\quad \times\Bigg[\exp\left(-K_{DR}\dot{z}\left(t-t_0\right)\right) \\ &\quad\quad -\exp\left(-\left(t-t_0\right)/\tau_{DR}\right)\Bigg] \\ &\quad +Q\left(t=t_0\right)\exp\left(-\left(t-t_0\right)/\tau_{DR}\right). \end{aligned} \tag{12}$$

To the best of our knowledge, Eq. (12) is new. By using this analytic expression for the pulmonary blood flow at arbitrary depths in Eq. (6), we very significantly decrease both the computational complexity and computer time needed for these calculations. The way this equation is implemented in practice for the full dive profile is briefly as follows. Operationally, one replaces $t_0 \to t_k$, $z(t) \to z_k\left(t,t_k\right)$, and $\dot{z} \to \dot{z}_k$ for each segment of the dive profile, where t_k is the time at which the k-th segment begins. Then $z\left(t,t_k\right) = z_k\left(t=t_k\right) + \dot{z}_k\left(t-t_k\right)$ is the expression which gives the depth at all times "t" for the k-th segment, and $\dot{z}_k$ is the constant ascent/descent rate of each k-th segment in the profile.

2.3. Tissue partial pressure of Nitrogen

In order to evaluate the tissue partial pressure of dissolved Nitrogen in each of the brain and the inner ear over the course of the breath-hold dive, we adopt a very simple mono-exponential compartmental model for each tissue-type [14, and references therein]. That is, we will have one such compartment for each of the brain and the inner ear. This simplified two-compartment independent parallel model of the head is illustrated in Fig. 3.

For this model, the Nitrogen partial pressure in each compartment is obtained during and after the breath-hold dive by integrating Eq. (13) [14, and references therein]:

$$\frac{P_T}{dt} = \frac{1}{\tau_T}\left(P_a(t) - P_T(t)\right). \tag{13}$$

Here the first-order time constant for each compartment is related to the compartment's half-life through $\tau_T = t_{1/2}/\ln 2$. The specific values used (that are shown in Fig. 2), were taken from [15]. The term $P_a(t)$ is obtained using Eq. (6). Because of the form of Eq. (6), Eq. (13) can only be integrated numerically.

2.4. Final working expressions for the rate of change of the bubble radius

The expression for the time evolution of a bubble's radius depends on the physical environment wherein the gas exchange between the bubble and it's the environment occurs. Specifically, if the bubble is traveling along an artery, the time-evolution of the radius is found by using Eq. (5) in Eq. (3) with $P_x = P_a$. In this case, P_a is obtained using

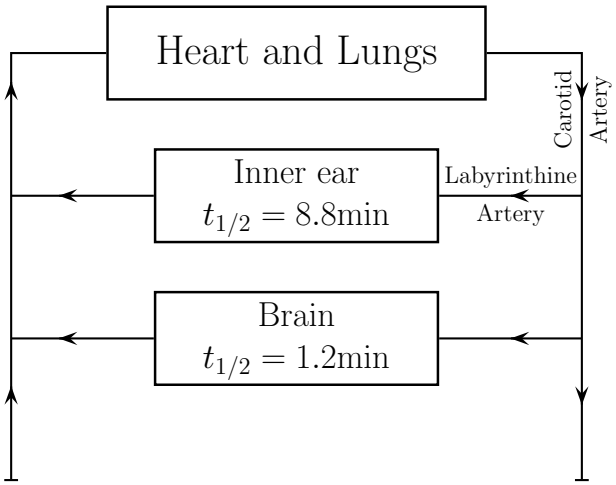

Figure 3: Independent parallel compartmental model of the head showing the brain and inner ear, each represented as independent mono-exponential compartments, with their respective half-lives ($t_{1/2}$).

Eq. (6), together with Eqs. (7), (8), and (12). Combining these equations gives

$$\frac{dR}{ds} = \frac{2s}{3P_eR^2+4\gamma R}\left\{3Dd\left(P_aR-P_eR-2\gamma\right)-R^3\dot{z}\right\}, \tag{14}$$

where we have defined

$$d \equiv \frac{BT}{KH}. \tag{15}$$

On the other hand, for a bubble lodged in a capillary surrounded by a supersaturated tissue whose dissolved Nitrogen partial pressure (P_T) is given by the solution of Eq. (13), P_x in Eq. (5) is now given by $P_T(t)$. Substituting Eq. (5) with $P_x = P_T(t)$ into Eq. (3) gives the following differential equation for the time-evolution of the bubble radius for the bubble lodged in a capillary

$$\frac{dR}{ds} = \frac{2s}{3P_eR^2+4\gamma R}\left\{3Dd\left(P_TR-P_eR-2\gamma\right)-R^3\dot{z}\right\}. \tag{16}$$

Note that Eq. (14) and (16) differ only by whether the arterial Nitrogen partial pressure (P_a), or the tissue Nitrogen partial pressure (P_T), is used for the dissolved Nitrogen partial pressure in the environment of the bubble (*i.e.*, in the bubble's WSR).

In order to solve Eq. (16) for the radius R, we first numerically integrate Eq. (13) with a 4th-order Runge-Kutta method [16] to provide values at time points on a one-dimensional grid. We then use these grid points, together with a simple linear interpolation scheme, to obtain the tissue Nitrogen tension P_T, at any required arbitrary time t. The interpolated function allows us to use a 4th-order Runge-Kutta method to solve for $R(t)$. This procedure significantly saves computational time since, by using it, we don't have to numerically integrate Eq. (13) at each time step of the Runge-Kutta algorithm.

Symbol	Value	Definition or explanation
γ	$0.7\ \text{atm} \cdot \mu$	Surface tension of water.
D	$2900 \frac{\mu^2}{\text{sec}}$	Diffusion constant of Nitrogen in water at 37 °C
T	37°C	Human body temperature
K_H	$1614 \frac{\text{atm} \cdot l}{\text{mol}}$	Henry's constant for Nitrogen in water at 37 °C
β	0.017/atm	Solubility of Nitrogen in blood at 37 °C
X_{N_2}	0.79	Mole fraction of Nitrogen in air
D_0	$\frac{0.456l}{\text{atm} \cdot \text{sec}}$	Capillary diffusing capacity of Nitrogen at surface
α	0.0018	Fitted constant (see Eq. (9) and Ref. [2])
τ_{DR}	8sec	See Eq. (10) and Ref. [2]
K_{DR}	0.01524/fsw	See Eq. (10) and Ref. [2]
Q_o	$\frac{3l}{\text{sec}}$	Minimum pulmonary blood flow
Q_s	$\frac{8l}{\text{sec}}$	Pulmonary blood flow at surface
$\tau_{T(\text{Brain})}$	$\frac{72}{\ln 2}$ sec	Time constant, single compartment model for the brain [15]
$\tau_{T(\text{Innerear})}$	$\frac{528}{\ln 2}$ sec	Time constant, single compartment model for the inner ear [15]

Table 1: Parameter values used

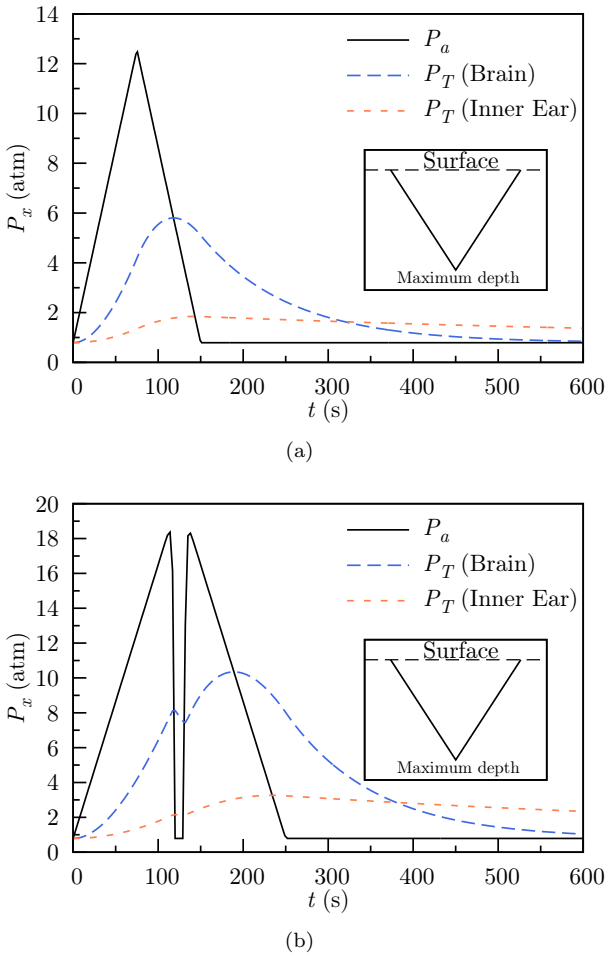

Figure 4: Partial pressures of dissolved Nitrogen in arterial blood, and in simple models of the inner ear and the brain during a breath-hold dive (a) without, and (b) with lung collapse. The insets are schematic representations of the "dive profile". The plots were determined from Eq. (6) and (13) for P_a and P_T, respectively, together with parameter values in Table 1, and details given in the text.

3. Results

The numerical values of the constants used in the equations are entered in Table 1.

Our results are given graphically in Sections 3.1 and 3.2, for single and repetitive breath-hold dives, respectively. The dive profiles used in these sections are roughly representative of those done in modern competitive breath-hold diving, and in commercial pearl diving.

3.1. Competitive-level single (non-repetitive) breath-hold dives

Fig. 4 illustrates how the dissolved Nitrogen partial pressures of arterial blood, and of (simplified models of) inner ear and brain tissue, vary over the course two single competitive-level breath-hold dives. The dives shown in Fig. 4(a) and 4(b) are to depths of 150 m and 250 m, respectively, and the descent and ascent rates were 2 m/sec.[2]

[2]Dives to such depths, and these rapid ascent/descent rates, are made with the assistance of specialized sleds and buoyancy devices that are used to speed the descent and ascent, respectively.

In Fig. 4(b) lung collapse occurs at ∼234m (117sec into the dive), and lung re-inflation occurs, on ascent, at ∼232m (134sec into the dive).

These plots clearly illustrate how tissues lag arterial blood with respect to their on- and off-gassing during compression and decompression, respectively. As indicated previously in Section 1.4, it is this lag that causes body tissues to become temporarily supersaturated with dissolved inert gas during the decompression phase of a dive. The dissolved inert gas partial pressure of arterial blood (in the absence of lung collapse) responds essentially instantaneously to changes in the depth or the ambient pressure. This explains the discontinuity in the slope of the P_a plot in Fig. 4(a) at 150 sec, which is the time at which the diver in Fig. 4(a) surfaces. Fig. 4(a) also illustrates the extent of supersaturation both of brain and inner ear tissue with respect to arterial blood, at various times after surfacing. Since the brain is a "faster" tissue than the in-

ner ear ($t_{1/2} = 72$ sec for the brain, *vs.* $t_{1/2} = 528$ sec for the inner ear), it will fill faster with inert gas during the compression part of the dive. Consequently, at the time of surfacing, the brain is seen to be more supersaturated than the inner ear. But this order is reversed at $\sim$ 325 s (or 3.42 min after surfacing) due to faster off-gassing of the brain during decompression at the surface. This explains why, at 600 sec from the start of the dive (8 min after surfacing), the brain is no longer supersatutated, but the inner ear still is.

As shown in Fig. 4(b), lung collapse is accompanied by a precipitous drop in the arterial gas partial pressure. It drops, in this model, to the whole body venous gas partial pressure, for the time during which the diver remains below $\sim$233 m. The whole body venous gas partial pressure is assumed here (as in [2]) to be unchanged from its surface value, and the basis for this assumption is the relatively short duration of a single breath-hold dive. While the effect of lung collapse on the arterial gas partial pressure is major, its net effect on the tissue dissolved gas pressures is fairly minor. Its effect on the latter is seen as a minor blip on the P_T plots in Fig. 4(b). The effect on P_T is minor because of the very short amount of time that the diver's lungs are totally collapsed in this dive ($\sim$ 15 sec).

Fig. 5 illustrates the evolution of AGEs, both before and after they enter the capillary networks of the brain and inner ear, during the decompression phase of a single breath-hold dive. Here the ascent and descent rates are 2 m/sec, and the maximum depth is 100 m. The three plots to the left of the solid vertical line show three AGEs dissolving in the main arteries due to the effect of surface tension. Their initial radii, defined here as their radii at the time they enter the left atrium of the heart, were taken to be 5μ, 10μ and 15μ. These AGEs, which may have resulted from a r/l shunt such as a PFO or an AVA, or from inadequate filtering of VGEs by the lungs, are assumed to enter the diver's left atrium at a depth of 8 m (or 4 sec before surfacing), during the diver's ascent to the surface. The time for the AGE to get to the head from the left atrium is approximately 3 sec [1], which is the time interval shown from the start of these plots to the solid vertical line in Fig. 5. It is seen that the 5μ and 10μ AGEs both dissolve before reaching the head, but the 15μ AGE survives the trip, arriving at one or other of the capillary networks with a radius of $\sim 9\mu$.

As seen from the plots to the right of the solid vertical line, the degree of supersaturation either of the brain or the inner ear, for this dive, is sufficient to cause the AGE radius to increase by a factor of $\sim 3 - 18$, depending on the tissue, and on what is assumed for the local (or effective) diffusion coefficient of dissolved Nitrogen in this region. Since capillaries are $O(10)\mu$ in diameter, AGEs that become inflated to this extent would be more than large enough to block the capillaries and cause ischemia. Conceivably, they may also cause the capillaries in which they are lodged to rupture, since capillary walls are extremely thin — their thickness is the same as the diameter of an epithelial cell.

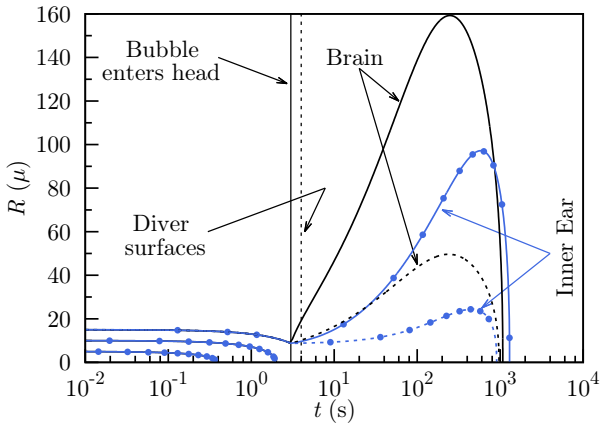

Figure 5: Time evolution of the bubble radius before and after the bubble enters the capillary networks in the brain and the inner ear. For the curves to the left of the solid vertical line, the diffusion coefficient (D) given in Table 1 was used. The solid and dashed curves to the right of the solid vertical line are for the diffusion coefficient (D) given in Table 1, and for 1/10 this value, respectively. The plots for R, before and after the bubble enters the head, were determined using Eq. (14) and (16) respectively, together with the relevant parameter values in Table 1, and details in the text.

Unfortunately, not much is known about how its diffusion coefficient is changed when the dissolved Nitrogen is in extra-vascular soft tissue, or in a capillary wall, as opposed to when it is in arterial blood. On physical grounds, one would expect some reduction in the value of its local (or effective) diffusion coefficient. For illustrative purposes then, in the plots to the right of the sold vertical in Fig. 5, we assumed two rather different values of the diffusion coefficient of dissolved Nitrogen: its value in water at body temperature (2900 $\mu^2\text{sec}^{-1}$, entered Table 1, which is also used for the AGE-in-an-artery calculations), and one-tenth this value. It is seen from the dashed plots to the right of the solid vertical in Fig. 5, that a reduction by an order-of-magnitude in the value of D, still results in a very significant degree of inflation of an AGE in the capillaries of these tissues.

The inflated AGEs finally dissolve in a little over 1000 sec, relative to the start of the dive, in the networks of the brain and inner ear. The final dissolution of the AGE occurs after the excess Nitrogen has been fully eliminated ("washed-out") from these tissues. The dissolution effect of surface tension is then re-established, and the bubble dissolves.

Figure 6 shows the relevant Nitrogen partial pressures that qualitatively account for the bubble's variation in radius, plotted previously in Fig. 5. Both here, and in Figs. 7-9, below, we use an intermediate value ($D/2$), for the effective diffusion coefficient of dissolved Nitrogen for the bubble-in-a-capillary calculations.

In Fig. 6, the increase in the bubble pressure before it reaches the head is due to the effect of surface tension

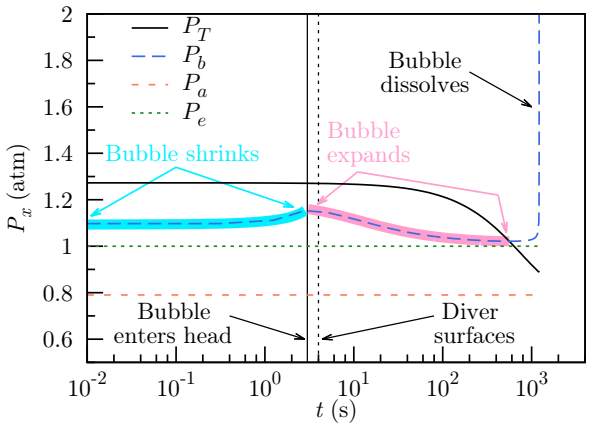

Figure 6: Arterial Nitrogen partial pressure (P_a), bubble pressure (P_b), ambient pressure (P_e), and tissue Nitrogen partial pressures for the inner ear (P_T). The bubble pressure shown is for the R (initial)=15μ bubble in Fig. 5. The effective diffusion coefficient within the inner ear tissue was here taken to be $D/2$, using the value of D entered in Table 1, and the plots were determined as in the caption to Fig. 4.

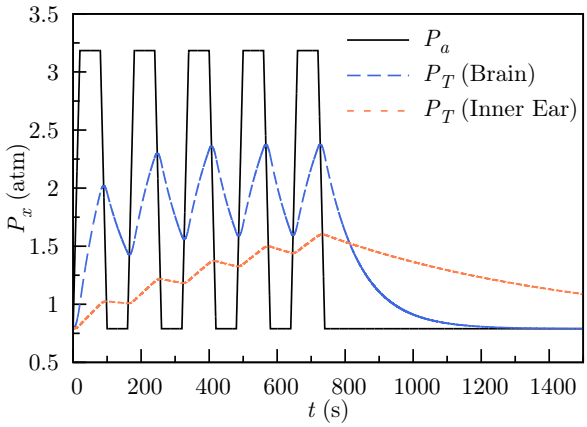

Figure 7: Arterial and tissue partial pressures of Nitrogen for a sequence of five repetitive breath-hold dives. The effective diffusion coefficient was taken to be $D/2$ within each tissue. The plots were determined as in the caption to Fig. 4, and details in the text.

that causes the bubble to shrink in this region (see Eq. (1)). Obviously, the inner ear tissue dissolved Nitrogen partial pressure has no influence on the bubble at this stage. However, when the bubble reaches the head (which is essentially when it also reaches the inner ear) the inflating effect of the contiguous supersaturated tissue takes effect. This effect exceeds the effect of surface tension, and the bubble begins to inflate. This occurs because (as shown in the figure) $P_T > P_b$ from the time the bubble enters the head, until the 563 sec point. At this time the pressures reverse in relative magnitude, and the bubble dissolves, both because of surface tension, and because, at this stage $P_T < P_b$.

3.2. Repetitive breath-hold dives

Fig. 7 illustrates the progressive dissolved Nitrogen pressure build-up in inner ear and brain tissue, with increasing numbers of repetitive dives. Each dive shown extends from the surface to a maximum depth of 100 fsw, at a descent rate of 300 fsw/min, followed by a time of 1 min at the maximum depth. The diver then ascends directly to the surface at an ascent rate of 300 fsw/min, and the surface interval between the repetitive dives is 1 min.

The Nitrogen build-up is seen to be noticeably greater for the inner ear than for the brain, and this can be understood from the characteristic on/off-gassing times of the two tissues ($t_{1/2}$ = 1.2min and 8.8min for the brain and inner ear, respectively). The surface interval is the phase of the dive during which most of the dive's decompression and tissue off-gassing occurs [14]. The 1 min surface interval used here, is sufficient for the brain to mostly (but not quite completely) eliminate its excess dissolved Nitrogen, but it isn't nearly enough for the inner ear to do so. Consequently, with progressively more dives, one gets a significant Nitrogen buildup for the inner ear, but only a slight build-up for the brain.

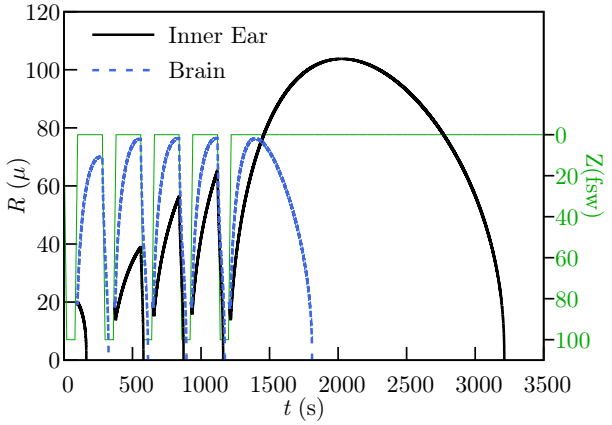

Figure 8: Gas bubble growth and dissolution in the brain and the inner ear for a series of five repetitive breath-hold dives. The green plot (whose scale is given on the right vertical axis) gives the depth as a function of time. The plots for R were determined as in the caption to Fig. 5, and details in the text. The effective diffusion coefficient was $D/2$.

The effect on the growth and dissolution of an AGE lodged in capillaries surrounded by these tissues is illustrated in Fig. 8 for a similar series of repetitive dives as was shown in Fig. 7. Here the bubble travels within the arterial system for 3 seconds before reaching the head, and the initial radius of the AGE (its radius in the left atrium at the start of the ascent from the first dive) is 20μ. The individual dives were again to 100 fsw, with ascent/descent rates of 300 fsw/min, but here the surface interval between dives was 3 min. It is seen that each bubble grows and shrinks with each ascent and descent, respectively, and that the maximum radius for the bub-

ble in the inner ear (attained during each surface interval) grows considerably with each progressive dive in the series. The growth and the maximum bubble radius in the brain are much more constrained, and again, this can be understood from the different off-gassing half-times of the brain and the inner ear. Evidently, the 3 min surface interval is nearly sufficient to off-gas the excess Nitrogen from the brain ($t_{1/2}$ = 1.2min), prior to each subsequent repetitive dive, but this is not the case for the inner ear ($t_{1/2}$ = 8.8min).

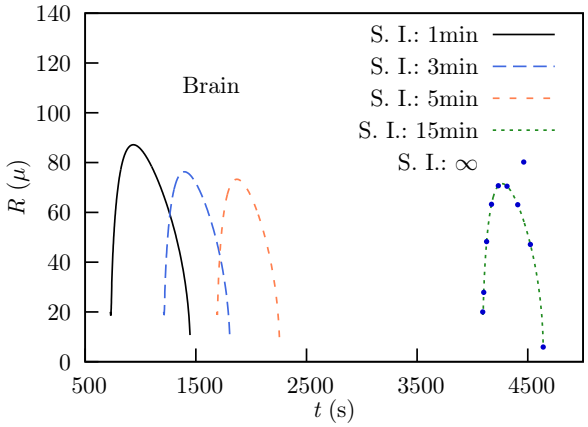

(a)

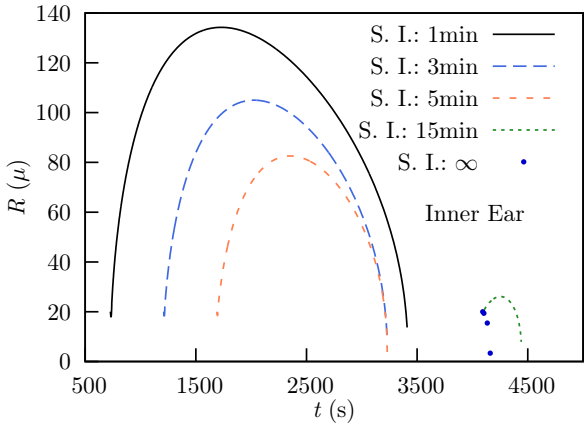

(b)

Figure 9: The effect of the duration of the surface interval on bubble growth and dissolution for a series of repetitive breath-hold dives, for (a) the brain and (b) the inner ear. The plots shown with solid or dashed curves are ***all*** for the 5$^{\text{th}}$ dive in a series of five dives, using different surface intervals between dives, for each series of dives. The plots shown with solid points (S.I. = ∞) are for the first dive in the series, with its time axis translated, so that its start coincides with the start of the 5$^{\text{th}}$ dive in the 15 min SI series. The plots were determined as in the caption to Fig. 5 and details in the text, and the effective diffusion coefficient was $D/2$.

In Fig. 9, we illustrate the effect of the duration of the surface interval, for dive profiles similar to those shown in Fig. 8. The dive profiles and initial bubble radius were the same as those for Fig. 8, except that here we vary the duration of the surface interval from one series of dives to the next. For example, the plots shown for SI = 1 min and 3 min in Fig. 9(a), represent the growth and dissolution of an AGE (in a capillary in the brain), in the 5$^{\text{th}}$ dive of a series of 5 dives, for which the surface intervals between the repetitive dives were 1min and 3 min, respectively.

It is seen from Fig. 9(a), that for the brain, a surface interval of 15 min is sufficient to totally eliminate dissolved Nitrogen buildup from the prior dives in the series. This is shown by the essentially exact coincidence of the plots for the 1$^{\text{st}}$ and 5$^{\text{th}}$ dive in the 15 min SI series. It is what would be expected for a fast tissue such as the brain ($t_{1/2}$ = 1.2 min) being allowed an off-gassing time of 15 min during each surface interval.

On the other hand, we see from Fig. 9(b), that a surface interval of 15 min is almost, but not quite sufficient, to totally eliminate dissolved Nitrogen build-up over this series of five repetitive dives for inner ear tissue. Again this is to be expected, since for the inner ear ($t_{1/2}$ = 8.8 min) a 15 min surface interval will eliminate most, but not quite all the Nitrogen that has built up in previous dive(s). Nevertheless, the difference between the extent of bubble inflation between the 1$^{\text{st}}$ and 5$^{\text{th}}$ dive is seen to be quite modest, for the 15 min SI series. Consequently, a 15 min surface interval should be almost enough to eliminate the increased risk (relative to a non-repetitive dive) of Inner Ear DCS for the repetitive breath-hold dives shown here.

These results are consistent with the experience of the pearl divers of the Tuamotu Archipelago, who learned from experience, that "Taravana" commonly occurred when the surface interval between dives was very short (*e.g.* 1 min), but that 15 min surface intervals were sufficient to prevent it (Introduction).

4. Summary

We solved the Laplace equation for a simple three-region diffusion model of a gas bubble in arterial circulation during and after a breath-hold dive. We determined the size and gas pressure within the bubble, for the bubble's arterial conduit in the presence and absence of contiguous supersaturated tissue. The bubble tends to shrink and dissolve (due to the effect of surface tension) when remote from supersaturated tissue, but, for a sufficient degree of tissue supersaturation, it will inflate significantly when near such tissue.

We applied our results to two types of breath-hold dives: single, very deep, competitive-level dives, and repetitive breath-hold dives similar to those carried out by a group of indigenous commercial pearl divers in the South Pacific. Our results were qualitatively consistent with what is known about DCS in breath-hold diving, for both types of dives.

Specifically, our model calculations predict that for the competitive-level single dives, both Cerebral and Inner Ear DCS are expected to occur occasionally, since the degree of supersaturation of both these tissues will be significant

on surfacing from dives involving these types of profiles. While the dataset for such dives is sparse, it was in fact the case that competitive-level breath-hold divers occasionally (several %) experienced symptoms suggestive of both Cerebral and Inner Ear DCS following their dives [2].

For the repetitive breath-hold dives of the kind done in commercial pearl diving, the duration of the surface interval between dives was found to be crucial. For surface intervals of $\sim$ 1 min, both Cerebral and Inner Ear DCS can be expected to occur, not infrequently, due to the significant build-up of excess Nitrogen in these tissues over a series of such repetitive dives. But the incidence of both forms of DCS is expected to drop very significantly for surface intervals of $\sim$ 15 min, or more. This is in line with the reported experience of the Tuamotuan breath-hold pearl divers.

Acknowledgements

We are grateful to the Natural Sciences and Engineering Research Council of Canada (NSERC) for financial support in the form of a Discovery Grant to one of us (SG).

References

References

[1] J.M. Solano-Altamirano, S. Goldman, The lifetimes of small arterial gas emboli, and their possible connection to Inner Ear Decompression Sickness, Math. Biosci., 252 (2014) 27.

[2] J.R. Fitz-Clarke, Risk of decompression sickness in extreme human breath-hold diving, Undersea Hyper Med., 36 (2009) 83.

[3] M. Ferrigno, C.E. Lundgren, In: Bennett and Elliott's Physiology and Medicine of Diving (5th ed), Edited by A.O. Brubakk and T.S. Neuman. Saunders 2003. Chapter 5.

[4] R.R. Pearson, G.H. Pezeshkpour, A.J.Dutka, Cerebral involvement in decompression sickness, Undersea Biomed Res., 19(suppl) (1992) 39.

[5] T.J.R. Francis, S.J. Mitchell, In: Bennett and Elliott's Physiology and Medicine of Diving (5th ed), Edited by A.O. Brubakk and T.S. Neuman. Saunders 2003. Chapter 10.4.

[6] R.E. Moon, E.M. Camporesi, J.A. Kisslo, Patent Foramen Ovale and Decompression Sickness in Divers, The Lancet 333, Issue 8637 (1989) 513.

[7] C. Klingmann, Inner Ear Decompression Sickness in Compressed-Air Diving, Undersea Hyperb. Med. 39 (1) (2012) 589.

[8] E. Cantais, P. Louge, A. Suppini, P.P. Foster, B. Palmer, Right-to-Left Shunt and Risk of Decompression Illness with Cochleovestibular and Cerebral Symptoms in Divers: Case Control Study of 101 Consecutive Dive Accidents. Crit. Care Med. 31 (2003) 84.

[9] E.R. Cross, Taravana - Diving Syndrome in the Tuamotu Diver, In: Physiology of Breath-hold Diving and the Ama of Japan. National Academy of Science - Nationasl Research Council Publication 1341 (1965) 207.

[10] R.M. Wong, Taravana Revisited. Decompression illness after breath-hold diving, South Pacific Underwater Medicine Society (SPUMS) Journal 29 (1999) 126.

[11] M. Ljubkovic, J. Zanchi, T. Breskovic, J. Marinovic, M. Lojpur, Z. Dujic, Determinants of Arterial Gas Embolism After Scuba Diving, J. Appl. Physiol. 112 (2012) 91.

[12] R.D. Vann, Inert Gas Exchange and Bubbles (Chapter 4), and Mechanism and Risks of Decompression Sickness (Chapter 7). In: Diving Medicine (4th ed), Edited by A.A. Bove and J.C. Davis. Saunders 2004.

[13] J.A. Jacquez, Compartmental Analysis in Biology and Medicine (2nd ed). The University of Michigan Press (1985) Chapter 10.2.

[14] S. Goldman, A New Class of Biophysical Models For Predicting the Probability of Decompression Sickness in Scuba Diving. J. Appl. Physiol. 103 (2007) 484.

[15] S. J. Mitchell, D.J. Doolette, Selective vulnerability of the inner ear to decompression sickness in divers with right to left shunt: the role of tissue gas supersaturation. J. Appl. Physiol. 106 (2009) 298.

[16] W.H. Press, B P. Flannery, S.A. Teukolski, W. Vetterling. Numerical Recipes, The Art of Scientific Computing (FORTRAN Version), Cambridge University Press, 1989. 548.